The effect of permeability on the erosion threshold of fine-grained sediments

Henning Mohr[1], Postdoctoral fellow, PhD

Scott Draper [2], Associate Professor, PhD

David J. White [3], Professor, PhD

Liang Cheng [4], Professor, PhD

ABSTRACT

The erosion of marine sediments, although difficult to predict, can lead to important implications in offshore engineering, sedimentology and coastal management. Continued research is, therefore, warranted to compile high-quality erosion data from which to develop models to better predict the erosion resistance of different types of marine sediments. In this paper, dimensional analysis is performed to express the threshold shear stress as a function of a selection of soil properties that are commonly linked to the erosion process of sediments. To identify the dominant dimensionless group, an experimental investigation on the erosion threshold was carried out using fine-grained sediments that were systematically prepared to ensure variations in (i) particle size distribution (i.e. fines content), (ii) bulk density, and (iii) hydraulic permeability. The samples included silica, carbonate and marine sediments, each of which are expected to have limited or no clay-mineral content. The measurements were analysed and compared with existing literature and

[1]Ocean Graduate School, The University of Western Australia, 35 Stirling Highway, Crawley, WA6009, Australia. E-mail: henning.mohr@uwa.edu.au.

[2]School of Civil, Environmental and Mining, The University of Western Australia, 35 Stirling Highway, Crawley, WA6009, Australia. E-mail: scott.draper@uwa.edu.au.

[3]University of Southampton, University Road, Southampton, SO171BJ, United Kingdom. E-mail: david.white@soton.ac.uk.

[4]School of Civil, Environmental and Mining, The University of Western Australia, 35 Stirling Highway, Crawley, WA6009, Australia. E-mail: liang.cheng@uwa.edu.au.

predictive models. It was found that marine sediment samples with limited fines content showed good agreement with the empirical Shields curve, irrespective of particle size distribution, bulk density and permeability. In contrast, for finer marine sediment it was found that variations in these soil properties modify the threshold shear stress away from the Shields curve. Across each of these parameters only permeability appeared to independently correlate with the observed range of threshold measurements. Motivated by this finding, a model is introduced to predict the threshold shear stress as a function of permeability and the reference erosion rate that is used to define when the threshold is reached. The resulting expression is shown to quantitatively explain the experimental data and is found to also agree with existing data from the literature for quartz sediments with a wide range in fines content. An apparent advantage of the new model is that it is consistent with existing studies that identify variations in threshold shear stress due to changes in bulk soil parameters – including fines content and bulk density – since each of these parameters also affect permeability.

INTRODUCTION

In coastal and offshore engineering, the prediction of sediment erosion is fundamental to the design of offshore structures, such as foundations and pipelines that are placed on the seabed. This is because ocean currents, tidal currents and waves can initiate sediment transport around the structure, leading to scour and significant changes in the local bathymetry. In turn, these changes can alter the hydrodynamic loading and geotechnical resistance; affecting the stability of the structures. Outside of offshore engineering, the prediction of sediment erosion is also important, for example, in the fields of environmental engineering, sedimentology and coastal management.

Motivated by the importance of predicting sediment erosion, numerous previous studies have focused on predicting the threshold shear stress of different sediments. The majority of this work has focused on sediments with individual grains that are well-rounded and uniformly graded, for which the well-known Shields curve typically gives a reasonable prediction of the threshold of erosion described by the dimensionless threshold Shields parameter (Shields 1936; Miller et al. 1977; Soulsby and Whitehouse 1997; Vanoni 2006). In comparison with these commonly studied sediments, natural marine sediments can be comprised of irregular shaped grains and may be widely graded, being composed of a range of particle sizes (Mehta 2013). Fine-grained sediments have also been found to exhibit very different threshold shear stress to that predicted using the Shields curve (see, for example, Whitehouse et al. 2000; Winterwerp and van Kesteren 2004; Torfs 1995; Grabowski et al. 2011). In particular, Mohr et al. (2013) showed significant differences in threshold shear stress compared with Shields curve predictions for silty sand and sandy silt recovered from the North West Shelf of Australia.

For sediments exhibiting higher threshold shear stress than predicted by the Shields curve, the increase in threshold shear stress has been traditionally attributed to the bulk properties of

the sediment if it has significant fines content (i.e. more than $\sim$10% by mass of sediment finer than 63 μm; Whitehouse et al. 2000). For example in the case of sediments with significant fines content including particles much smaller than 63 μm, it has been shown experimentally that the threshold shear stress is dependent on bulk density (which is linked to the state of consolidation) and the particle size distribution or fines content (see, for example, Paphitis 2001; Lick and McNeil 2001; Torfs 1995; Panagiotopoulos et al. 1997). These finer sediments are also often sticky to the touch and cling together when moist. For this reason they are commonly referred to in the literature as 'cohesive' sediments (Whitehouse et al. 2000; Winterwerp and van Kesteren 2004) which suggests that cohesive bonds between particles are also a contributing factor. However, it should be noted that particles in sediments with low permeability may cling together when moist or saturated because of negative pore pressure, irrespective of cohesive bonds. Additionally, many sediments, including marine sediments, may have predominantly fine non-clay mineral particles; Mehta (2013) notes that due to their low specific area fine non-clay mineral particles do not display significant cohesion.

More recently, Winterwerp (2012) suggests that turbulent stresses on a particle may induce local negative pore pressure (i.e. suction) which is dependent on the rate of deformation (i.e. erosion rate) and the seepage flow within the bed (i.e. permeability). In line with this suggestion, Mohr et al. (2018) presents a set of experimental results on the erosion behaviour of fine-grained reconstituted marine sediments showing that permeability is the only soil parameter that showed a consistent correlation with observed erosion trends produced by variations in the bulk properties of the sediments.

Based on the literature above, the measured shear stress (denoted as τ'_{cr} in this paper) may be related to the following set of variables if cohesive bonding is neglected (e.g. for sediment with no

or limited clay-mineral content and no biological bonding)

$$\tau'_{\mathrm{cr}} = f\left(\rho,\ \nu,\ d_{50},\ \left(\rho_s - \rho\right)\mathrm{g},\ \rho_{\mathrm{bulk}},\ \mathrm{Fines},\ k,\ \eta'_{\mathrm{cr}}\right). \tag{1}$$

The first four parameters on the right hand side of Eq. (1) are commonly used for non-cohesive sediments and include the fluid density ρ, the fluid kinematic viscosity ν, the median grain diameter d_{50}, and the submerged specific weight given in terms of the density of the sediment ρ_s, the fluid density ρ and acceleration due to gravity g. The next three parameters in Eq. (1) represent the bulk properties of the sediment, with ρ_{bulk} defining the bulk density, Fines the fines content and k the hydraulic conductivity. The last parameter in Eq. (1) is the reference erosion rate of the sediment at threshold (η'_{cr}) and is equal to the volume of sediment per unit area and time being removed at threshold from the sample (i.e. the flux of sediment being removed at threshold). Typically this rate will not be equal to zero, since most studies (e.g. Vanoni 1964; Miller et al. 1977; Buffington and Montgomery 1997; Roberts et al. 1998; Paphitis 2001) define threshold to occur when the erosion rate or transport rate exceeds some small measurable value (as discussed later, in this study threshold is defined to occur when the erosion rate first exceeds 10^{-7} m/s; e.g. $\eta'_{\mathrm{cr}} = 10^{-7}$ m/s). Equation (1) does not explicitly include the shape of the particles, or the fabric of the sediment, but the effect of these properties on tortuosity is encapsulated through k. The sediments tested and compared in this paper consider a wide range of particle shape (from angular marine sediment to rounded quartz), but it will be shown that this does not appear to effect the ability of the parameters in (1) to explain the measured threshold shrear stress.

Noting that there are three primary dimensions, Eq. (1) can be re-written as

$$\frac{\tau'_{\mathrm{cr}}}{(\rho_s-\rho)gd_{50}} = \theta'_{\mathrm{cr,s}} = f\left(\mathrm{Re}_{\mathrm{d}_{50}} = \frac{u_{*,\mathrm{cr}}d_{50}}{\nu},\ \frac{\rho_{\mathrm{bulk}}}{\rho},\ \mathrm{Fines},\ \mathrm{Re}_{\mathrm{k}} = \frac{u_{*,\mathrm{cr}}\sqrt{k}}{\sqrt{\nu \mathrm{g}}},\ \frac{\eta'_{\mathrm{cr}}}{k}\right), \qquad (2)$$

where θ'_{cr} is the non-dimensional threshold shear stress and $u_{*,\mathrm{cr}} = \sqrt{\frac{\tau'_{\mathrm{cr}}}{\rho}}$ is the critical friction velocity. The four parameters on the right hand side of Eq. (2) represent the grain Reynolds number ($\mathrm{Re}_{\mathrm{d}_{50}}$), a non-dimensional bulk density, the (already) dimensionless fines content, the permeability Reynolds number (Re_{k}) and a relative erosion rate (akin to the ratio of deformation to seepage flow within the sediment).

The aim of this paper is to explore the functional relationship in Eq. (2). For fine sediments (and for all those tested herein) the permeability Reynolds number is often significantly less than unity, implying that the flow is laminar within the sediment itself (Voermans et al. 2017); hence variations in this parameter are not expected to alter the flow regime within the soil matrix. This paper therefore presents a set of experiments on artificial and marine sediments that explore in detail how the remaining four dimensionless groups in Eq. (2) correlate with threshold shear stress. The experimental results are also compared with existing empirical models (including the Shields curve) and existing findings in the literature. Based on these comparisons, the underlying experimental results and dimensional analysis, a novel predictive model based on dimensional reasoning is introduced that considers erosion as a rate dependent process, accounting for hydraulic permeability. This model suggests that a suction force (defined in terms of the erosion rate and soil permeability) should be considered in the force balance on a given particle. Due to the addition of this suction force, the dimensionless expression predicts that the measured threshold shear stress for fine sediments may be higher than the empirical Shields curve by an amount that depends

on the hydraulic permeability of the sediment and the reference erosion rate that is used to define threshold shear stress. Both parameters appear to control the trends in the experimental results. The proposed model has been calibrated based on data from this study and is subsequently compared to independent experimental data from the wider literature.

As noted later in the paper, threshold shear stress and the erosion rate close to threshold may be interpreted in terms of a probability of erosion (see e.g. Mehta 2013 and the references cited therein). This idea is not pursued further in this paper, but would be a useful area of further work to expand on the results herein. In this paper a focus is placed on correlating mean shear stress with bulk soil properties.

EXPERIMENTAL PROCEDURE

Sediment characterisation

Three groups of sediments have been investigated in this study, including (i) three marine sediments sourced from the North West Shelf of Australia, (ii) two uniform silica sands and (iii) one artificial carbonate silt. The Particle Size Distribution (PSD) for each sediment is presented in Fig. 1 and specific information on the PSD and specific gravity are given in Table 1.

The three marine sediments in Table 1 represent a Silty SAND (NWS1), a Very Silty SAND (NWS2) and a Sandy SILT (NWS3), respectively. Most particles for these sediments are non-symmetric, exhibiting rough and smooth surface textures and irregular shapes (see Figure 4.2 in Mohr 2015). These underlying particle shapes give rise to a high range in voids ratio and, hence, a large permeability range. For all of the investigated marine sediments, for example, the voids ratio ranges from 0.8 to 1.8 which is typical for calcareous sediment on the NWS of Australia (see Jewell and Khorshid 1988). In comparison to the marine sediments, the two silica sands (SS1 and

SS2) and carbonate sediment (CS1) exhibit almost uniform particle size distribution (Fig. 1) and give rise to a voids ratio range between 0.5 to 0.8. Both SS1 and SS2 are comprised of smooth rounded particles, whereas CS1 particles exhibit a regular crystalline shape (see Figure 4.2 in Mohr 2015). The silica and artificial carbonate sediment have no clay-mineral content, whilst all three of the marine sediments are expected to have no or limited clay mineral content, in line with other marine sediments that have been recovered from the North West Shelf of Australia (e.g. Lehane et al. 2014). Reconstitution of the marine sediments has also removed the likelihood of biological bonding.

Experimental setup

The erosion tests were performed in a recirculating flume, which comprises a horizontal fully enclosed circulating water channel and includes a rectangular test section with dimensions 1.8 m (length) $\times$ 0.3 m (high) $\times$ 0.2 m (wide) (see Figure 2 and Mohr et al. (2016a) for more details). The sediments were prepared in a semi-cylindrical sample holder of diameter 72 mm and length 150 mm. The holder was placed in a cavity at the bottom of the test section so as to lie horizontally flush with a false floor (in a similar way to that described by Mohr et al. 2013). The roughness of the false floor was adjusted to best match the roughness of the individual samples. Initial experiments were carried out to determine the hydrodynamic shear stress acting on the sample which consisted of measuring the streamwise velocity profile near the bed at the location of the sample. The measurements taken with an Acoustic Doppler Velocimeter (Nortek Vectrino Profiler) were consistent with a logarithmic profile having the form

$$U(z) = \frac{u_*}{0.4} \ln\left(\frac{z}{z_0}\right), \tag{3}$$

where z is the height above the sample surface, U is the streamwise velocity above the bed and u_* is a friction velocity related to the seabed shear stress. The parameter z_0 in Eq. (3) is a roughness length obtained by fitting to the measurements. Across the different roughness scenarios, this length agreed well with the empirical formula given by Christoffersen and Jonsson (1985) and resulted in a calculated shear stress with an accuracy of $\pm 2\%$ (see Mohr et al. 2016a). More details on the shear stress measurements can be obtained from Mohr (2015).

In order to measure erosion rates, a steady shear stress of $\sim$0.02 Pa was first generated in the flume and then increased in a stepwise manner every 3 minutes, in increments of $\sim$0.04 m/s measured at 35 mm above the bed. After each interval, any observation of sediment movement was noted and a 3D surface scan of the sample was recorded. The assessed scan area covered 80% of the total sample surface to avoid the influence of edge effects in the measurements. Using the scan measurements, an apparent erosion rate (η) was calculated by dividing the measured incremental erosion depth, averaged over the sample area, by the time increment of the applied shear stress. This apparent erosion rate therefore accounts for all sediment removed from the sample. For fine sediments in which transport along the bed is negligible, η is equal to the true erosion rate divided by one minus the porosity of the sample (see, e.g. Mohr et al. 2016b, Section 3.3). Due to spatial variations across the eroded sample, different sized averaging areas showed fluctuations in erosion rates within $\pm 5\%$. In addition to the step tests, supplementary tests were undertaken to measure the erosion depth every 30 seconds under steady flow conditions. The erosion rates were then obtained from the initial slope on a plot of the mean erosion depth as a function of time. The erosion rate was initially constant, but began to reduce with depth due to hydrodynamical shielding of the sample or an increase in erosion resistance with depth. To avoid any influence of depth dependent effects on the erosion rate, erosion rates in the step tests were only measured provided the cumulative erosion

depth was sufficiently small to negate shielding effects. Measurements from the supplementary testing for the same experimental setup and sediments as that adopted here are presented in Mohr et al. (2016b).

In the present study, the threshold shear stress was defined as the point when the erosion rate of the sample exceeded an apparent erosion rate below 10^{-7} m/s (or 0.36 mm/hr), which was the smallest value the scanning system could reliably measure. Initial movement of the sample occurs simultaneously at many locations across the sample surface, the average erosion rate gives a good indication of the mean shear stress when sediment movement is significant, and minimises some of the effects associated with instantaneous stresses due to turbulence (Paintal 1971).

As noted in the introduction, defining threshold using a finite erosion rate is consistent with that used or suggested by other researchers (e.g. Vanoni 1964; Miller et al. 1977; Buffington and Montgomery 1997; Roberts et al. 1998; Paphitis 2001). For a coarse sediment that moves only in bedload transport, control volume arguments can be used to relate an apparent erosion rate of 10^{-7} m/s to a dimensionless transport rate of between 10^{-4} and 10^{-3} for sandy sediment, depending on the erosion sample length (see, e.g. Mohr et al. 2016b, Section 3.3). This range in transport rate is consistent with that adopted by Smith and Cheung (2004) and can be related to early studies such as Kramer (1935) as weak transport. Finally based on our definition, the threshold shear stress estimates for the silica sands used in this study were in very good agreement with the well-known Shields curve (see also Mohr 2015).

It should be noted that the erosion rate close to threshold may also be interpreted in terms of a probability of erosion (see e.g. Mehta 2013 and the references cited therein). This idea is not pursued further in this paper, but would be a useful area of further work.

Experimental schedule

A total of 36 individual erosion tests were carried out in order to investigate the influence of soil properties of the sediment on the threshold shear stress.

Firstly, a set of experiments focused on the influence of bulk density on threshold shear stress. Table 2 shows the range of bulk densities tested with each of the sediments. For the artificial sediments, the loosest densities were produced by natural settling and the denser ones by shaking the soil for 1 minute. For the finer marine sediments, the soil was mixed with different quantities of water to obtain different densities.

Secondly, another set of experiments focused on the influence of particle size distribution and fines content on threshold shear stress. To undertake these experiments, the marine sediments were sieved into particle fractions smaller and larger than 75 μm and then recombined in different ratios to achieve the fines contents listed in Table 3.

Thirdly, a number of experiments focused on the measurement of permeability to investigate the influence of permeability on the threshold shear stress. Tests conducted in Table 2 were linked with permeability measurements.

Sample preparation

Each sediment sample subjected to erosion testing was prepared in a specific and repeatable way. For sediments that did not have any fine fraction, traditional wet pluviation (see Donahue et al. 2008) was adopted. Using this method, a slurry of material was poured into a large tub and allowed to settle naturally. Subsequent coring was then undertaken using the sample holder to create the test sample. In contrast, sediments with a significant fine fraction were mixed to a thick slurry (to maintain a homogeneous mixture) using a measured quantity of water and together

with consolidation weights a target density was achieved. Sample holders with sediment having no fine fraction were rested for at least one hour prior to erosion testing, whereas finer sediments were allowed 24 hours to settle. Samples were then levelled (if necessary) with a plastic scraper to ensure a flat surface was present for erosion testing and carefully placed in the recess of the false floor in the flume.

Water content measurements were obtained before and after testing. To obtain the water content before the test, a second identical sample was prepared for water content measurement. The water content after the test was taken from the sample itself. Since erosion is a surface phenomenon, care was taken to only sample within the first 20 mm from the surface and at three locations across the sample. Measurements showed that the sample preparation method was repeatable (to within $\pm 1\%$ in water content) and that differences in the water content measurements before and after the test were generally small (1–2%) across all samples.

RESULTS AND DISCUSSION

Fig. 3 gives an example set of results for two samples, namely NWS2-T1 and NWS3-T1. In this figure, post processing of the 3D surface scans has been used to calculate an apparent erosion rate and this has been used to determine threshold shear stresses of 0.32 Pa and 0.96 Pa, respectively, using the reference erosion rate of $\sim 10^{-7}$ m/s.

To indicate how the sediment eroded, Fig. 3 also shows profiles of the two samples (taken lengthwise through the sample) at different times during the experiments. It can be seen that there are differences in the erosion patterns for the two samples, and this was a result of differences in the mode of erosion. More specifically, for sample NWS2-T1 particles were observed to move grain-by-grain in bedload transport following initiation of motion. As a result, erosion initiated

generally at the upstream edge of the sample, leading to uneven erosion across the sample as the shear stress increased (i.e. compare Profile 1 with Profile 3). In contrast, for sample NWS3-T1 the flume became cloudy very quickly following threshold conditions, indicating entrainment into suspension. As a result, erosion was observed to occur uniformly across the sample at shear stresses close to threshold, indicative of Profile 1 and Profile 2. However at higher shear stresses (above $\sim$1.7 Pa), the erosion of small clumps of particles was observed. These clumps moved in a sporadic fashion and led to a more irregular erosion profile, as can be seen in Profile 3.

The observations for the samples included in Fig. 3 were representative of the range in erosion modes observed across all of the different marine and artificial sediments tested. More specifically, at shear stresses close to threshold conditions the uniform silica sands (SS1 and SS2), the carbonate sediment (CS1), and two of the marine sediment (NWS1 and NWS2), were found to move mainly as bedload transport in a similar manner to NWS2-T1. These samples tended to move particle-by-particle and displayed preferential erosion at the upstream edge of the sample. For the finer sediments, and in particular each of the NWS3 sediments tested, the water became cloudy at shear stresses just above the threshold shear stress indicating that fine particles had been entrained and washed from the surface of the sample. This initial erosion process appeared to be a continuous and uniform process and is consistent with the mechanism of surface erosion described by, for example, Torfs (1995). At higher shear stresses, surface erosion was accompanied by the abrupt removal of clumps of sediment, which appeared to resemble the process of mass erosion described by Winterwerp and van Kesteren (2004).

Median particle size

In Fig. 4 the non-dimensional threshold shear stresses for all of the samples are plotted as a function of dimensionless grain size, which is defined as

$$D_* = \left[\frac{\mathrm{g}(\frac{\rho_s}{\rho} - 1)}{\nu^2}\right]^{1/3} d, \tag{4}$$

where g is the acceleration due to gravity, ρ_s is the grain density, ρ is the fluid density, ν is the kinematic viscosity of the fluid and d is the grain size. The density and the viscosity of the water are taken to be 1000 $\mathrm{kg/m^3}$ and 1.003 $\times$ 10^{-6} $\mathrm{m^2/s}$, respectively, in all calculations.

As outlined by Soulsby and Whitehouse (1997), the dimensionless grain size is a convenient parameter to use when calculating threshold shear stress and it can be written as a function of the grain Reynolds number and the Shields parameter, e.g.

$$D_* = ({\mathrm{Re}_{\mathrm{d}_{50}}}^2/\theta)^{(1/3)}. \tag{5}$$

Hence, Fig. 4 explores the relationship between threshold shear stress and the first non-dimensional parameter in Eq. (4).

Fig. 4 also shows a modified Shields curve together with data compiled by Soulsby and Whitehouse (1997), as well as the data for quartz sediments obtained from Roberts et al. (1998). The modified Shields curve is defined by Soulsby and Whitehouse (1997) as

$$\theta_{\mathrm{cr,s}} = \frac{0.3}{1 + 1.2D_*} + 0.055\left[1 - \exp\left(-0.020D_*\right)\right]. \tag{6}$$

Based on the data shown in Fig. 4, it can be seen that regardless of density or particle size

the threshold shear stresses of the artificial sediments SS1, SS2 and CS1 are in agreement with the Shields curve, lying well within the scatter of the data compiled by Soulsby and Whitehouse (1997). Since these sediments are similar in particle shape and size to sediments that have been used to define the Shields curve, these results confirm the suitability of the experimental testing setup, as well as the measurement of shear stress and the underlying definition of the threshold shear stress. In contrast to the artificial sediments, Fig. 4 shows some differences in threshold shear stress between the Shields curve and marine sediments tested in this study. Such differences are also apparent in the results presented from Roberts et al. (1998). In both set of data the modified Shields curve appears to indicate a lower limit for the threshold shear stress of finer sediments.

Bulk density

The first set of experiments focused on sediments prepared at different bulk densities. This set of experiments was motivated by the many previous studies which have shown that increases in threshold shear stress are correlated with increases in bulk density for fine sediments having mean particle sizes smaller than 50–100 μm and a significant fraction of fines (e.g. Torfs 1995; Roberts et al. 1998; Briaud et al. 2001; Lick et al. 2004; Partheniades 2009). These previous studies having considered both artificial mixtures and natural sediments (Postma 1967, Williamson and Ockenden 1992; Mitchener et al. 1996; Jepsen et al. 1997; Roberts et al. 1998; Houwing 1999; Lick and McNeil 2001). Of particular note within this collection of studies is the work of Mitchener et al. (1996), who collected a comprehensive set of data for artificial mixed sediments (comprising sand-mud to mud-only mixtures) and fitted a relationship to explain threshold shear stress in terms of bulk density.

$$\tau_{\rm cr} = 0.015(\rho_{\rm bulk} - \rho)^{0.73}, \quad (7)$$

where $\rho_{\rm bulk}$ represents the bulk density and ρ is the density of water.

Fig. 5 presents the non-dimensional threshold shear stress measurements from Table 2 as a function of non-dimensional bulk density. Focusing on each sediment separately, it can be seen that there is a clear positive trend between density and threshold shear stress, in broad qualitative agreement with the existing literature. This trend is most noticeable for the marine sediments (and especially the finer marine sediment NWS3-T1). The trend is also noticeable for the artificial sediments, but the variation is less significant, and this is due, in part, to the fact that the artificial sediments only support small changes in density whilst the marine sediments support larger ranges in bulk density owing to their particle shape and distribution (Jewell and Khorshid 1988). Collectively, the two studies (from Roberts et al. 1998 and the present studies) together with Eq. (7) from Mitchener et al. (1996) confirm that threshold shear stress increases with bulk density. However, the functional relationship between threshold shear stress and bulk density is different for different sediments and is not generally well defined by Eq. (7).

Fines content

The fines content of the sediment is usually defined as the percentage of particles by mass with diameter less than some specified value. In many studies, this reference value is taken to be 63 μm (e.g. Torfs 1995; Roberts et al. 1998; Whitehouse et al. 2000, etc.) or 75 μm (e.g. Ye 2012; Mohr 2015). In this work 75 μm has been used in accordance with Australian Standards; however, the percentage fines content of the tested and analysed sediments are similar if 63 μm is used as the cut off instead.

With respect to the effect of fines content on threshold shear stress, various researchers have reported that the threshold shear stress increases steadily or abruptly with an increase in the fines content (Grissinger et al. 1981; Kamphuis and Hall 1983; Nalluri and Alvarez 1992; Lick et al. 2004; Mitchener et al. 1996; Van Ledden et al. 2004). The fines content at which significant changes in threshold shear stress occur have also been reported. For example Mitchener et al. (1996) observed a change of threshold shear stress at 3 to 15% fines content for artificially produced mixtures based on results from Torfs (1995) (comprising 3% for kaolinite, 7–13% for montmorillonite) and Alvarez-Hernandez (1990) (comprising 5–15% for laponite clay). Panagiotopoulos et al. (1997) observed a slow increase in threshold shear stress with mud content for a sand-mud mixture, before a sudden increase at around 30% mud content, whilst for natural mud mixtures Le Hir et al. (2008) presented a summary of results which indicated a significant increase in threshold shear stress at a mud content of 25–40%.

To compare with these earlier findings, Fig. 6 presents the dimensionless threshold shear stress as a function of fines content for the sediment samples listed in Table 3, together with additional data from Table 2. It is apparent in this figure that there is a general increase in threshold shear stress with fines content; however, the measured shear stress is also clearly dependent on bulk density. To illustrate this, a trend line of constant density has been drawn through the data for NWS2 (at a density of $\sim$1800–1850 $\mathrm{kg/m^3}$). Along this line it can be observed that below 50% fines content, a slight increase in shear stress threshold occurs with increasing fines content. In contrast, beyond 50% fines content a more rapid increase occurs. A line of constant density has also been drawn on Fig. 6 for the experimental data from Roberts et al. (1998) for a bulk density of 1850 $\mathrm{kg/m^3}$ (which is similar to that drawn for NWS2). It can be seen that for Roberts et al. (1998) the threshold shear stress changes only slightly for fines contents less than 80%, before increasing

slightly towards a fines content of 100%.

For the marine sediments NWS1 and NWS3, there is insufficient data to draw similar lines of constant density; however, the slope of the trend lines in Fig. 6 suggest that the fines content also influences the threshold shear stress for those sediments (i.e. NWS3, which has a higher fines content, has a much stronger correlation with density than NWS1).

Collectively, the two lines drawn in Fig. 6 indicate that at similar bulk densities, the relationship between threshold shear stress and fines content is different for different sediments. This implies that, as was the case for bulk density, the fines content does not appear to independently explain the threshold shear stress across different sediments. Instead, the effects of fines content coupled with density can be seen to effect the threshold shear stress.

A failure to appreciate that different sediment can have a different relationship between bulk properties and threshold shear stress may lead to an erroneous conclusion that the threshold shear stress reduces with reducing bulk density (if the fines content coincidently reduces) or increasing fines content (if the bulk density coincidently reduces).

Permeability

In previous studies (e.g. Winterwerp and van Kesteren 2004; Jacobs 2011), permeability was mentioned to be potentially a significant parameter for the erosion process. Furthermore, permeability appears to be closely related to sediment properties that are well-known to correlate with the threshold shear stress (e.g. bulk density and fines content) and it appears to be a physically reasonable parameter due to its influence on suction forces that may effect sediment mobility. However, despite these points, to date no systematic experimental study has been carried out to quantify the relationship between permeability and the erosion resistance of sediments. This is possibly due

to the fact that permeability is generally difficult to measure or estimate, especially, for the top layers in a soil (Jacobs 2011). Nevertheless, later in this paper it will be seen that often an order of magnitude estimate may be sufficient to quantify the effect of permeability on threshold shear stress.

A series of Rowe cell tests with consolidation steps in combination with constant head tests were carried out to determine the permeability of samples in Table 2 (see Whitlow 2001 for details). Fully saturated mixtures with consolidation stages of 20, 40, 80 and 160 kPa were modelled to prevent vertical movement of the sample and to enable testing across a range of densities. A vertical head difference of 10 kPa was applied over the soil sample. The upward flow rate was measured by means of the water outflow from the sample, and this was used to deduce the permeability. Fig. 7 presents measurements of permeability as a function of voids ratio (e) for each of the sediments tested. Based on this data, a relationship of the following form has been fitted for each of the sediments (following Mesri and Olson 1971):

$$\log(k) = a \log(e) + b, \tag{8}$$

where a and b are fitted coefficients. Eq. (8) was then used to estimate the permeability for each of the natural sediments (having different bulk density) subjected to erosion tests. To illustrate if this approximation required extrapolation or interpolation of the Rowe cell measurements, Fig. 7 shows the measured bulk densities (i.e. voids ratio) from the individual erosion tests on top of the fitted curves based on Eq. (8).

Fig. 8 shows the non-dimensional threshold shear stress and the ratio of reference erosion rate to permeability for the sediments in Table 2. Generally, there is a strong trend in the data, with

the erosion resistance increasing with reduced permeability for samples having permeability below 10^{-5} m/s (e.g. $\eta'_{\mathrm{cr}}/k > 10^{-2}$). This finding is consistent with trends observed for bulk density and fines contents in literature as permeability decreases with increasing bulk density and increasing fines content.

To further explore the relationship between permeability and threshold shear stress, a comparison is made with the results compiled by Roberts et al. (1998) for quartz sediments. Roberts et al. (1998) defined threshold shear stress for these sediments at an erosion rate of $\eta'_{\mathrm{cr}} = 10^{-6}$ m/s (Roberts et al. 1998, pp. 1263), but did not explicitly measure permeability. To approximate the permeability, the Kozeny-Carman equation has been used to compute the permeability as a function of the particle size distribution and density reported for each sample by Roberts et al. (1998). The use of the Kozeny-Carman equation is likely to be a reasonable approximation for quartz sediments (Mitchell and Soga 1979), and allows the permeability to be written as (after Chapuis and Aubertin 2003)

$$k = C_{\text{K-C}} \frac{\mathrm{g}}{\mu\rho} \frac{1}{S^2 G_{\mathrm{s}}^2} \left(\frac{e^3}{1+e} \right), \tag{9}$$

where $C_{\text{K-C}}$ is the Kozeny-Carman coefficient, g is gravity, μ is the dynamic viscosity of water (taken to be 1×10^{-3} Pa s throughout), S is the specific surface, ρ is the density of water, G_{s} is the specific gravity and e is the voids ratio. In this work, the constant $C_{\text{K-C}}$ was taken as 0.2, which is common for uniform spheres (Carman 1956). The specific surface (S) of fine-grained non-plastic soils was approximated based on the formula of Chapuis and Legare (1992).

$$S = 6/\rho_s \sum \left(\frac{P_{NoD} - P_{Nod}}{d} \right), \tag{10}$$

where $(P_{NoD} - P_{Nod})$ is the percentage by weight smaller than size D (P_{NoD}) and larger than the next size d (P_{Nod}).

Fig. 8 indicates a similar trend between permeability and threshold shear stress for the result from Roberts et al. (1998) to that observed for the marine sediments tested in the present study.

EROSION RATE-DEPENDENT MODEL TO PREDICT THRESHOLD SHEAR STRESS

From the results presented in Fig. 8, the relative permeability shows a strong correlation with threshold shear stress for sediment with significant fines content, whereas the Shields curve appears to correlate as expected with coarser sediments (see Fig. 4). Other soil properties (such as bulk density and fines content) do not independently explain the trends in the measured threshold shear stress. From a physical point of view, permeability is the only soil parameter which is related to hydraulic processes such as seepage beneath an eroding particle, and shows consistent correlative behaviour with most observed erosion threshold trends produced by variations in sediment properties, such as bulk density and fines content.

Assuming that bulk density and fines content influence the threshold shear stress because of their relationship with permeability, Eq. (2) can be simplified leading to:

$$\theta'_{\mathrm{cr}} \cong f(\mathrm{Re}_{d_{50}},\ \frac{\eta'_{\mathrm{cr}}}{k})\ . \tag{11}$$

Now, since the measured threshold shear stress limits to the modified Shields curve for coarse sediments (with relatively high permeability) and shows strong correlation with permeability for fine sediment, it is assumed that Eq. (11) can be simplified further to give:

$$\theta'_{\mathrm{cr}} \cong \theta_{\mathrm{cr,s}} + f\left(\frac{\eta'_{\mathrm{cr}}}{k}\right), \tag{12}$$

where $\theta_{\mathrm{cr,s}}$ is the predicted threshold shear stress based on the modified Shields curve (see Eq. (6)) and the function on the right hand side is assumed to be significant for large values of η'_{cr}/k and negligible for small values of η'_{cr}/k. The inclusion of $\theta_{\mathrm{cr,s}}$ in Eq. (12) effectively captures the dependence on grain Reynolds number ($\mathrm{Re}_{d_{50}}$).

Using the calculated permeability for each of the samples from Fig. 7 and noting that $\eta'_{\mathrm{cr}} = 10^{-7}$ m/s for the present erosion experiments, Fig. 9 presents the shear stress ratio $\theta'_{\mathrm{cr}}/\theta_{\mathrm{cr,s}}$ as a function of the non-dimensional parameter η'_{cr}/k for each of the sediments listed in Table 2. Eq. (12) is fitted to the experimental results using a linear relationship with a constant of proportionality of 7.7.

$$\frac{\theta'_{\mathrm{cr}}}{\theta_{\mathrm{cr,s}}} = 1 + 7.7\left(\frac{\eta'_{\mathrm{cr}}}{k}\right). \tag{13}$$

To further investigate if the model is able to predict the data from different studies, Fig. 10 compares Eq. (13) with the complete set of measured threshold shear stresses from Roberts et al. (1998) which were linked with estimated permeabilities using the Kozeny-Carman equation given in Eq. (9) (noting that Fig. 10 shows the prediction with $\eta'_{\mathrm{cr}} = 10^{-6}$ m/s). Very good agreement is observed between the measured data and the predictive formula given in Eq. (13), despite the fact that Roberts et al. (1998) used different sediment, and a different reference erosion rate. Fig. 11 presents the same threshold shear stress results from Fig. 10, but plotted against median grain size. Excellent agreement is obtained between the prediction from Eq. (13) and the measured data for median grain sizes ranging between 0.008 mm and 0.06 mm; hence, the model can accurately account for the unique non-linear trends with particle size for different bulk density. For very fine material, the predictions underestimate the threshold shear stress. This disagreement may be due

to limitations in the estimation of permeability using the Kozeny-Carman equation.

An important feature of the rate dependent model is that the reference rate of erosion defining threshold can significantly alter the measured threshold shear stress. This result implies that some of the scatter in existing experimental data for fine sediments may be simply due to differences in reference erosion rate. For example, the set of erosion rate curves given in Table 1 in Roberts et al. (1998) can be used to calculate the threshold at a reference erosion rate of 4×10^{-6} m/s (~ 15 mm/hr) leading to a noticeable increase in measured threshold shear stress. Existing theoretical models linking bulk properties to threshold shear stress are not able to explain this increase in threshold shear stress. However, as shown in Fig. 12, the rate dependent model introduced in this paper can predict this increase. Even though permeability might be considered a difficult parameter to measure (or estimate), the proposed model is not very sensitive to relatively small changes in permeability that might arise from measurement errors or assumptions. Furthermore, it provides excellent agreement between the two studies and follows general trends observed in literature (e.g. Torfs 1995; Ye 2012; Jacobs et al. 2011).

CONCLUSIONS

In this paper, a series of threshold shear stress measurements have been presented and compared with existing data and literature. Generally, it has been found that threshold shear stress for sediments with limited fines content agree well with the empirical Shields curve. Whilst for sediments with significant fines content the threshold shear stress exceeded the Shields curve prediction by up to an order of magnitude. To explain the increased threshold shear stress for the finer sediment, comparison has been made to measured soil properties such as bulk density, fines content and hydraulic permeability. Out of each of these soil properties only permeability appeared to

475 independently explain the increases in measured threshold shear stress across each of the sediment
476 types.

477 Motivated by the observed trend between threshold shear stress and permeability, dimensional
478 analysis has been used to develop a rate-dependent model to predict threshold shear stress. Fol-
479 lowing calibration of the model with the present experimental data, application of the model only
480 requires the Shields parameter (based on the particle size distribution) and both an erosion rate at
481 threshold and the permeability of the sediment. A comparison of the model with the independent
482 data compiled by Roberts et al. (1998) showed very good agreement, despite the fact that the data
483 from Roberts et al. (1998) was obtained for a different sediment type and relied on a different
484 reference erosion rate to define the threshold shear stress.

485 The rate-dependent model is also in good agreement with traditional models (i.e. Shields curve)
486 and reported erosion trends in literature. For example, density and particle size distribution both
487 affect the permeability of the soil, in a way that would lead to changes in threshold shear stress pre-
488 dicted by the model. Equally, changes in permeability may also explain trends observed by authors
489 who have suggested that the shape of particles, the plasticity index, and the orientation and fabric
490 of the sediment particles alter the threshold shear stress (Tavenas et al. 1983). The new model
491 also shows that the reference rate of erosion defining threshold condition can significantly alter the
492 measured threshold shear stress. This result implies that much of the scatter in existing experi-
493 mental data for fine sediments could be due to differences in reference erosion rate. Further work
494 is needed to investigate the physical arguments of the derived model expression that was obtained
495 using dimensional analysis. Further work is also needed to consider the effect of permeability on
496 the overall erosion resistance of fine-grained sediments with electrochemical cohesion.

ACKNOWLEDGMENTS

This research forms part of the activities of the Centre of Offshore Foundation Systems (COFS) which has been supported as a node of the Australian Research Council's Centre of Excellence for Geotechnical Science and Engineering (CGSE), and through the Fugro Chair in Geotechnics, the Lloyd's Register Foundation Chair and Centre of Excellence in Offshore Foundations and the Shell Chair in Offshore Engineering. Part of this research was conducted by the Wave Energy Research Centre and jointly funded by The University of Western Australia (UWA) and the Western Australian Government, via the Department of Primary Industries and Regional Development (DPIRD). The first author acknowledges his Research Studentship support from UWA. The first and second author acknowledge the support of the Lloyd's Register Foundation. The Foundation helps to protect life and property by supporting engineering-related education, public engagement and the application of research. The third author acknowledges the support of Shell, via the Shell Chair in Offshore Engineering at UWA. This research is supported through ARC Discovery Grants Program: DP130104535. All authors gratefully acknowledge the help provided by the anonymous reviewers of the paper.

REFERENCES

Alvarez-Hernandez, E. M. (1990). "The influence of cohesion on sediment movement in channels of circular cross-section." Ph.D. thesis, University of Newcastle, United Kingdom.

Briaud, J. L., Ting, F. C. K., Chen, H. C., Cao, Y., Han, S. W., and Kwak, K. W. (2001). "Erosion function apparatus for scour rate predictions." *Journal of Geotechnical and Geoenvironmental Engineering*, 127(2), 105–113.

Buffington, J. M. and Montgomery, D. R. (1997). "A systematic analysis of eight decades of incip-

519 ient motion studies, with special reference to gravel-bedded rivers." *Water Resources Research*,
520 33(8), 1993–2029.
521 Carman, P. C. (1956). *Flow of gases through porous media*. Butterworths Scientific Publications,
522 London.
523 Chapuis, R. P. and Aubertin, M. (2003). *Predicting the coefficient of permeability of soils us-*
524 *ing the Kozeny-Carman equation*. Technical Report (EPM-RT-200303), École Polytechnique de
525 Montréal.
526 Chapuis, R. P. and Legare, P.-P. (1992). "A simple method for determining the surface area of
527 fine aggregates and fillers in bituminous mixtures." *Effects of aggregates and mineral fillers on*
528 *asphalt mixture performance*, 1147, 177–186.
529 Christoffersen, J. B. and Jonsson, I. (1985). "Bed friction and dissipation in a combined current
530 and wave motion." *Ocean Engineering*, 12(5), 387–423.
531 Donahue, J. L., Bray, J. D., and Riemer, M. F. (2008). *Liquefaction susceptibility, resistance, and*
532 *response of silty and clayey soils*. Technical Report (UCB/GT 2008-01), University of Califor-
533 nia.
534 Grabowski, R. C., Droppo, I. G., and Wharton, G. (2011). "Erodibility of cohesive sediment: The
535 importance of sediment properties." *Earth-Science Reviews*, 105, 101–120.
536 Grissinger, E. H., Little, W. C., and Murphey, J. B. (1981). "Erodibility of streambank materials of
537 low cohesion." *Transactions of the American Society of Agricultural Engineers*, 24(3), 624–630.
538 Houwing, E.-J. (1999). "Determination of the critical erosion threshold of cohesive sediments on
539 intertidal mudflats along the Dutch Wadden Sea Coast." *Estuarine, Coastal and Shelf Science*,
540 49, 545–555.
541 Jacobs, W. (2011). "Sand-mud erosion from a soil mechanical perspective." Ph.D. thesis, Delft

University of Technology, Netherlands.

Jacobs, W., Le Hir, P., van Kesteren, W., and Cann, P. (2011). "Erosion threshold of sand-mud mixtures." *Continental Shelf Research*, 31, 14–25.

Jepsen, R., Roberts, J., and Lick, W. (1997). "Effects of bulk density on sediment erosion rates." *Water, Air, and Soil Pollution*, 99(1-4), 21–31.

Jewell, R. J. and Khorshid, M. S. (1988). *Engineering for calcareous sediments: North Rankin A foundation project state of the art reports*. Balkema, Rotterdam.

Kamphuis, J. W. and Hall, K. R. (1983). "Cohesive material erosion by unidirectional current." *Journal of Hydraulic Engineering*, 109(1), 49–61.

Kramer, H. (1935). "Sand mixtures and sand movement in fluvial models." *Transactions of the American Society of Civil Engineers*, 100, 798–878.

Le Hir, P., Cann, P., Waeles, B., Jestin, H., and Bassoullet, P. (2008). "Chapter 11: Erodibility of natural sediments: experiments on sand/mud mixtures from laboratory and field erosion tests." *Proc. in Marine Science*, 9, 137–153.

Lehane, B. M., Carraro, J. A. H., Boukpeti, N., and Elkhatib, S. (2014). "Mechanical response of two carbonate sediments from Australia's North West Shelf." *Proc. 33rd International Conference on Ocean, Offshore and Arctic Engineering*.

Lick, W., Jin, L., and Gailani, J. (2004). "Initiation of movement of quartz particles." *Journal of Hydraulic Engineering*, 130(8), 755–761.

Lick, W. and McNeil, J. (2001). "Effects of sediment bulk properties on erosion rates." *The Science of the Total Environment*, 266, 41–48.

Mehta, A. J. (2013). *An introduction to hydraulics of fine sediment transport*. World Scientific Publishing Company.

565 Mesri, G. and Olson, R. E. (1971). “Mechanisms controlling the permeability of clays.” *Clays and*
566 *Clay Minerals*, 19, 151–158.
567 Miller, M. C., McCave, I. N., and Komar, P. D. (1977). “Threshold of sediment motion under
568 unidirectional currents.” *Sedimentology*, 24(4), 507–527.
569 Mitchell, J. K. and Soga, K. (1979). *Fundamentals of soil behavior*. Wiley, New York.
570 Mitchener, H., Torfs, H., and Whitehouse, R. J. S. (1996). “Erosion of mud/sand mixtures.” *Coastal*
571 *Engineering*, 29, 1–25 (Errata, 1997, 30, 319).
572 Mohr, H. (2015). “Erosion and scour behaviour of marine sediments.” Ph.D. thesis, University of
573 Western Australia, Australia.
574 Mohr, H., Draper, S., Cheng, L., White, D. J., An, H., and Zhang, Q. (2016a). “The hydrodynamics
575 of a recirculating (O-tube) flume.” *Proc. 8th International Conference on Scour and Erosion*,
576 999–1010.
577 Mohr, H., Draper, S., and White, D. J. (2013). “Free field sediment mobility on Australia’s North
578 West Shelf.” *Proc. 32nd International Conference on Ocean, Offshore and Arctic Engineering*,
579 V04BT04A051, 11 pages.
580 Mohr, H., Draper, S., White, D. J., and Cheng, L. (2016b). “Predicting the rate of scour beneath
581 subsea pipelines in marine sediments under steady flow conditions.” *Coastal Engineering*, 110,
582 111–126.
583 Mohr, H., Draper, S., White, D. J., and Cheng, L. (2018). “A laboratory investigation into the
584 erosion rate of marine sediments.” *Coastal Engineering*, 140, 124–135.
585 Nalluri, C. and Alvarez, E. (1992). “The influence of cohesion on sediment behaviour.” *Water*
586 *Science and Technology*, 25(8), 151–164.
587 Paintal, A. S. (1971). “Concept of critical shear stress in loose boundary open channels.” *Journal*

588 *of Hydraulic Research*, 9(1), 91–113.

589 Panagiotopoulos, I., Voulgaris, G., and Collins, M. B. (1997). "The influence of clay on the thresh-
590 old of movement of fine sandy beds." *Coastal Engineering*, 32, 19–43.

591 Paphitis, D. (2001). "Sediment movement under unidirectional flows: an assessment of empirical
592 threshold curves." *Coastal Engineering*, 43, 227–245.

593 Partheniades, E. (2009). *Cohesive sediments in open channels: Erosion, transport and deposition*.
594 Butterworth-Heinemann, Oxford.

595 Postma, H. (1967). "Sediment transport and sedimentation in the estuarine environment." *Estuar-*
596 *ies*, 83, 158–179.

597 Roberts, J. D., Jepsen, R., Gotthard, D., and Lick, W. (1998). "Effects of particle size and bulk
598 density on erosion of quartz particles." *Journal of Hydraulic Engineering*, 124(12), 1261–1267.

599 Shields, A. (1936). "Anwendung der Aehnlichkeitsmechanik und der Turbulenzforschung auf die
600 Geschiebebewegung." Ph.D. thesis, Preußische Versuchsanstalt für Wasserbau und Schiffbau,
601 Germany.

602 Smith, D. A. and Cheung, K. F. (2004). "Initiation of motion of calcareous sand." *Journal of*
603 *Hydraulic Engineering*, 130(5), 467–472.

604 Soulsby, R. L. and Whitehouse, R. J. S. (1997). "Threshold of sediment motion in coastal envi-
605 ronments." *Proc. 13th Australasian Coastal and Ocean Engineering Conference and 6th Aus-*
606 *tralasian Port and Harbour Conference*, 1, 145.

607 Tavenas, F., Jean, P., Leblond, P., and Leroueil, S. (1983). "The permeability of natural soft clays.
608 part ii: Permeability characteristics." *Canadian Geotechnical Journal*, 20(4), 645–660.

609 Torfs, H. (1995). "Erosion of mud/sand mixtures." Ph.D. thesis, Katholieke Universiteit Leuven,
610 Belgium.

611 Van Ledden, M., van Kesteren, W. G. M., and Winterwerp, J. C. (2004). “A conceptual framework
612 for the erosion behaviour of sand-mud mixtures.” *Continental Shelf Research*, 24, 1–11.
613 Vanoni, V. (1964). “Measurements of critical shear stress for entraining fine sediments in a bound-
614 ary layer.” Ph.D. thesis, California Institute of Technology, United States.
615 Vanoni, V. A. (2006). *Sedimentation engineering*. American Society of Civil Engineers.
616 Voermans, J. J., Ghisalberti, M., and Ivey, G. N. (2017). “The variation of flow and turbulence
617 across the sediment-water interface.” *Journal of Fluid Mechanics*, 824, 413.
618 Whitehouse, R. J. S., Soulsby, R., Roberts, W., and Mitchener, H. (2000). *Dynamics of estuarine*
619 *muds*. Thomas Telford Publishing, London.
620 Whitlow, R. (2001). *Basic soil mechanics*. Prentice Hall.
621 Williamson, H. J. and Ockenden, C. M. (1992). *Tidal transport of mud/sand mixtures, laboratory*
622 *tests*. HR Wallingford, Report.
623 Winterwerp, J. C. (2012). “A conceptual framework for shear flow-induced erosion of soft cohesive
624 sediment beds.” *Journal of Geophysical Research*, 117, C10020.
625 Winterwerp, J. C. and van Kesteren, W. G. M. (2004). *Introduction to the physics of cohesive*
626 *sediment in the marine environment*. Elsevier, Amsterdam.
627 Ye, Z. (2012). “Erosion threshold and erosion rate of seabed sediments.” Ph.D. thesis, University
628 of Western Australia, Australia.

List of Tables

Sediment type	Abbreviation	Sediment type	d_{50} (mm)	Fines[1] (%)	Clay[2] (%)	G_s (–)
Marine sediments	NWS1	Silty SAND	0.31	7.5	0.9	2.78
	NWS2	Very Silty SAND	0.18	17.7	2.7	2.74
	NWS3	Sandy SILT	0.12	38.9	8.2	2.76
Artificial sediments	SS1	Coarse SAND	0.54	0	0	2.75
	SS2	Fine SAND	0.19	0	0	2.67
	CS1	Very fine SAND	0.08	46.9	0	2.71

[1] < 75 µm

[2] < 2 µm

TABLE 1: Properties of sediments tested.

Sample	Fines[1] (%)	d_{50} (mm)	ρ_{bulk} ($\mathrm{kg/m^3}$)	e (–)	τ_{cr} (Pa)
NWS1-T1	7.5	0.31	1890	1.00	0.21
			1928	0.92	0.26
			1928	0.92	0.31
			1956	0.86	0.36
			1971	0.83	0.42
NWS2-T1	17.7	0.18	1779	1.23	0.19
			1830	1.10	0.27
			1852	1.04	0.32
			1914	0.90	0.60
NWS3-T1	38.9	0.12	1624	1.82	0.26
			1670	1.63	0.55
			1691	1.55	0.61
			1707	1.49	0.61
			1715	1.46	0.74
			1731	1.41	0.96
SS1-T1	0	0.54	1974	0.79	0.25
SS2-T1	0	0.19	1986	0.69	0.16
			2001	0.67	0.16
CS1-T1	46.9	0.08	2036	0.65	0.15
			2090	0.57	0.18

[1] < 75 µm

TABLE 2: Threshold shear stress for sediments with varying bulk density.

Sample	Fines[1] (%)	d_{50}[2] (mm)	ρ_{bulk} ($\mathrm{kg/m^3}$)	τ_{cr} (Pa)
NWS1-T2	0	0.33	1877	0.22
	5	0.32	1877	0.22
	7.5	0.31	1928	0.26
	10	0.30	1928	0.26
	15	0.29	1915	0.35
	30	0.23	1843	0.33
NWS2-T2	0	0.22	1830	0.20
	5	0.21	1830	0.24
	10	0.20	1841	0.28
	15	0.19	1852	0.23
	17.7	0.18	1830	0.27
	30	0.14	1852	0.30
	50	0.075	1779	0.29
	100	0.026	1734	0.79
NWS3-T2	39	0.12	1707	0.61
	100	0.013	1739	0.84

[1] < 75 µm

[2] Calculated diameter based on changes in fines content

TABLE 3: Threshold shear stress for sediments with varying particle size distribution.

List of Figures

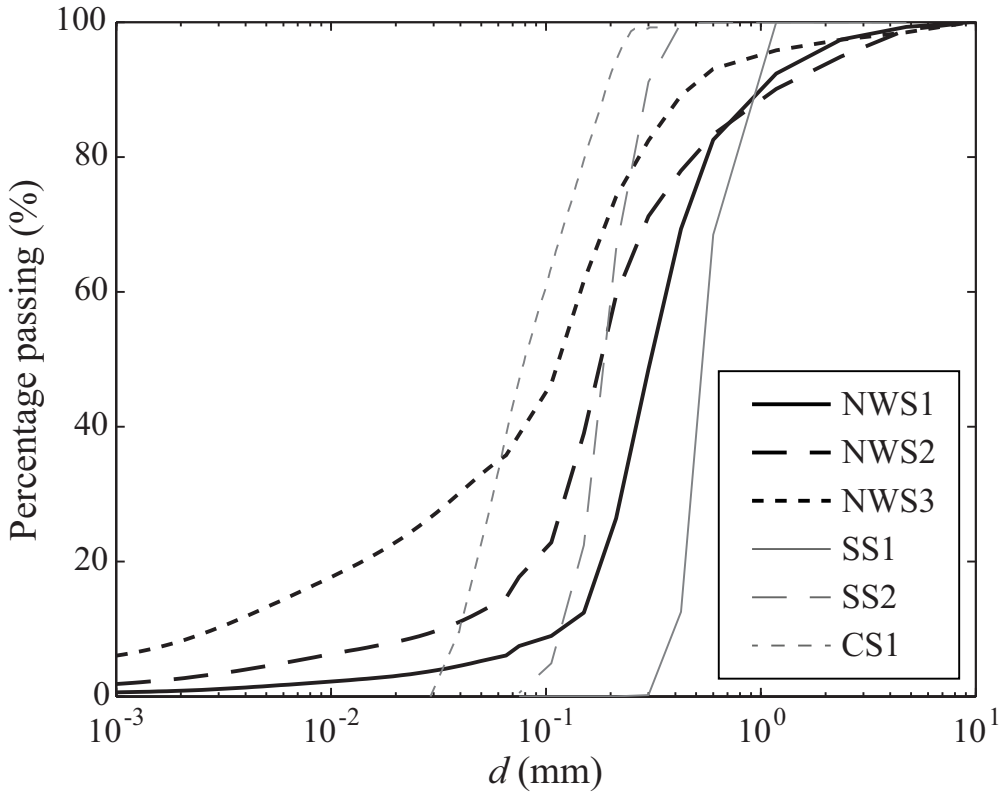

FIG. 1: Particle size distribution for tested sediments.

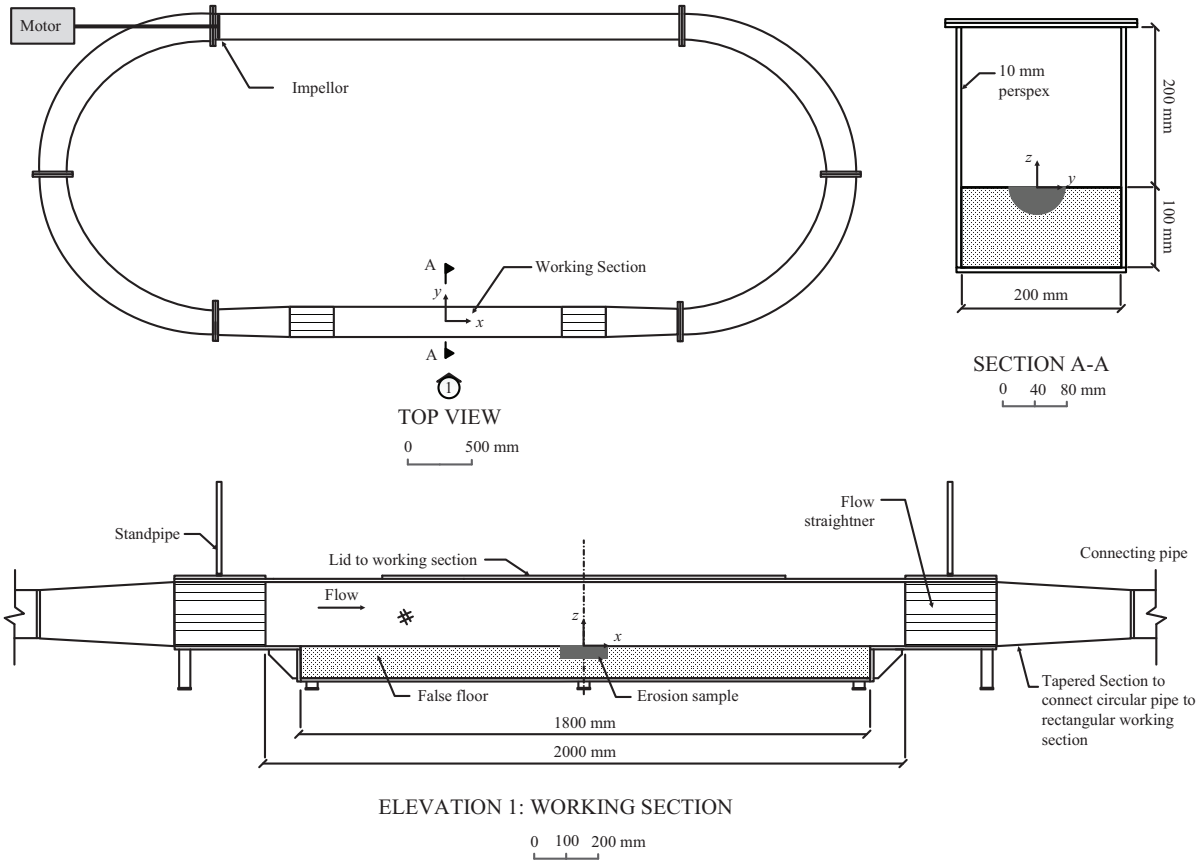

FIG. 2: Detailed dimensions of the recirculating flume comprising the erosion setup.

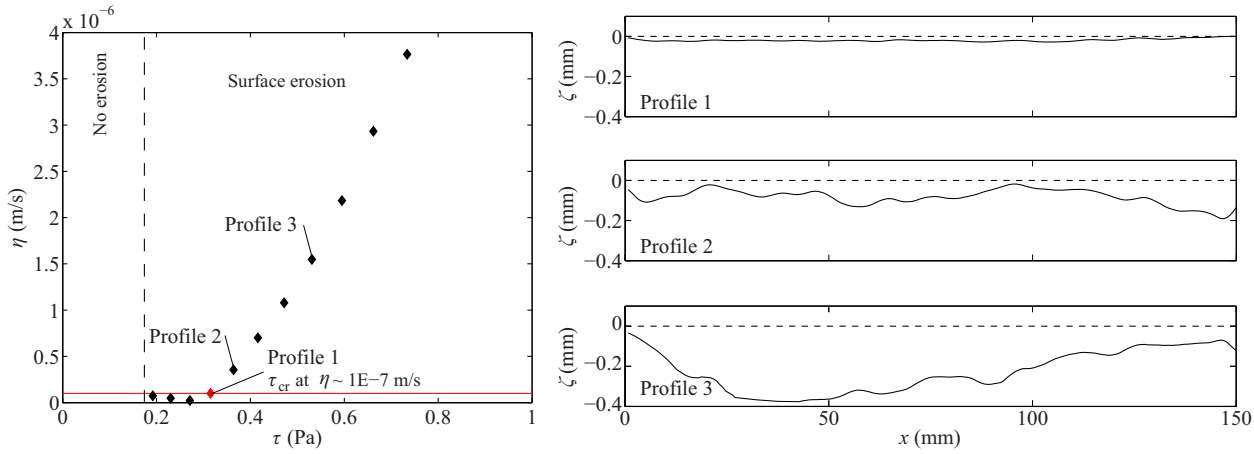

(a) Sample NWS2-T1 with $\rho_{\mathrm{bulk}} = 1852$

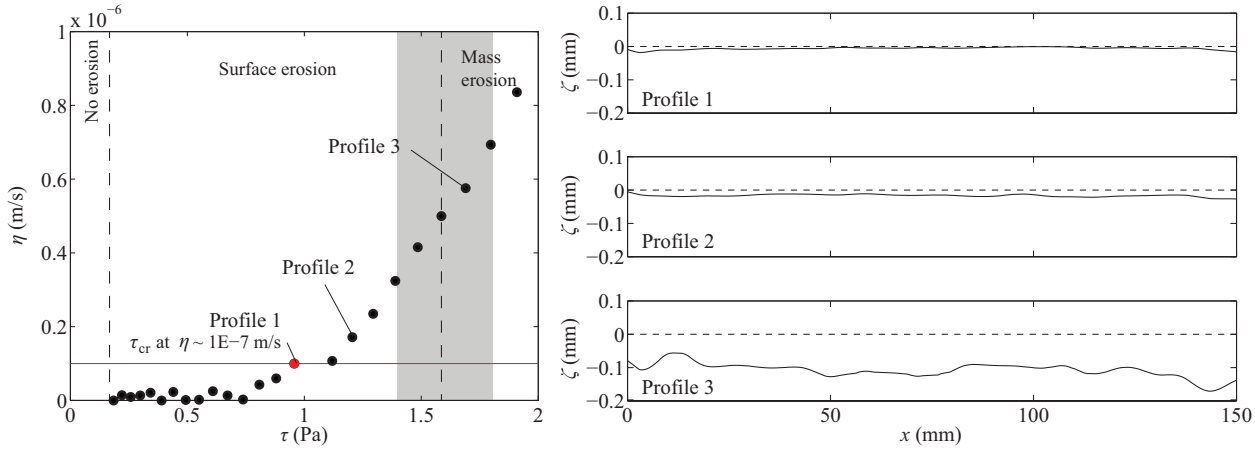

(b) Sample NWS3-T1 with $\rho_{\mathrm{bulk}} = 1731$

FIG. 3: Erosion rate data with the respective plots of erosion depth profile (ζ) (at the centre position) of the sample for (a) NWS2-T1 (very silty SAND) and (b) NWS3-T1 (sandy SILT). Also shown is the determination of the threshold shear stress at an erosion rate of 10^{-7} m/s and the observed erosion mechanism across the tested shear stress range.

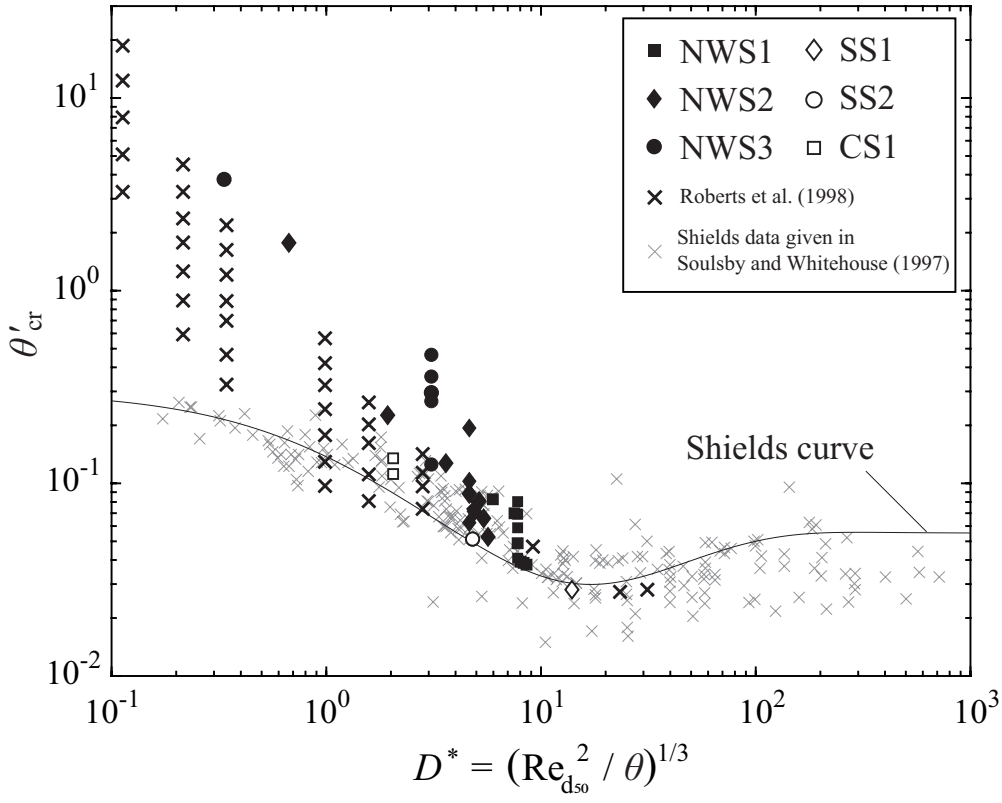

FIG. 4: Dimensionless threshold shear stresses of all tested sediments and data from Roberts et al. (1998) in comparison with the Shields curve and scatter after Soulsby and Whitehouse (1997). The diameters used in this figure vary slightly from the original ones as they were calculated from digitised PSD curves given in Roberts et al. (1998).

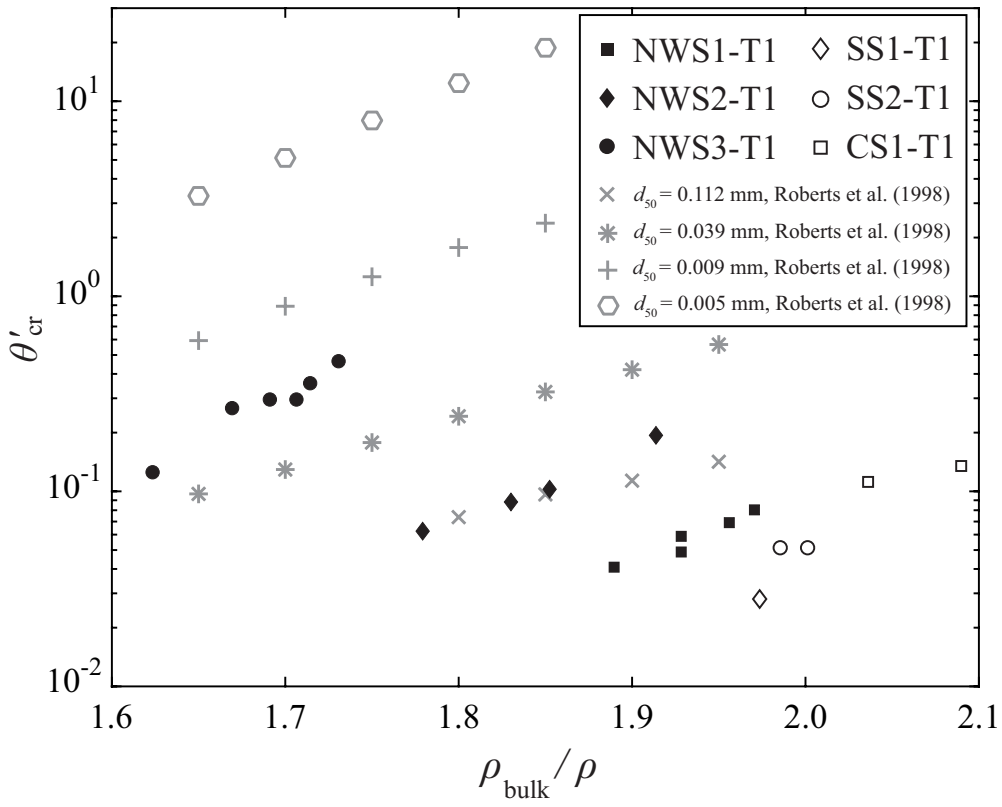

FIG. 5: Effect of density variation on dimensionless threshold shear stress considering tests in Table 2 and a selection of quartz sediments from Roberts et al. (1998). The diameters used in this figure vary slightly from the original ones as they were calculated from digitised PSD curves given in Roberts et al. (1998).

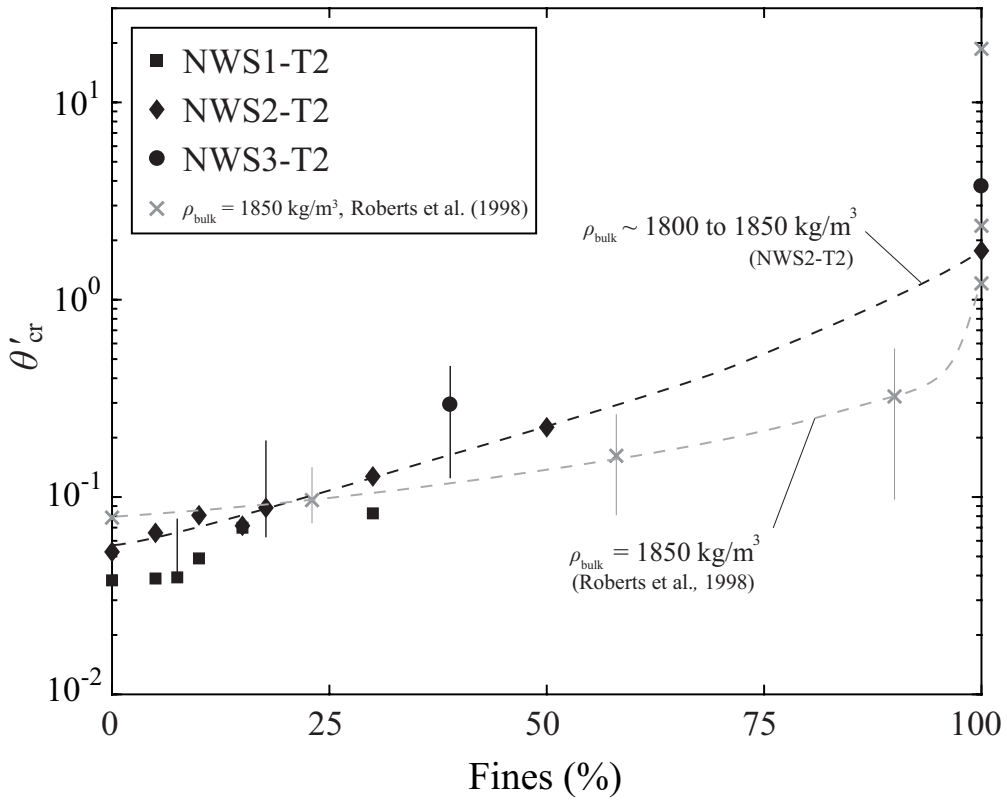

FIG. 6: Effect of fines content on dimensionless threshold shear stress with data from Table 3. Changes in threshold due to density variation from Table 2 are indicated in form of vertical lines. Also shown are data points for quartz sediments from Roberts et al. (1998) with $\rho_{\mathrm{bulk}} = 1850\ \mathrm{kg/m^3}$ (vertical lines indicate variations due to density). Black line indicates trend line for NWS2-T2 at $\rho_{\mathrm{bulk}} \sim 1800$–$1850\ \mathrm{kg/m^3}$ and grey line represents interpolation assuming $\rho_{\mathrm{bulk}} = 1850\ \mathrm{kg/m^3}$.

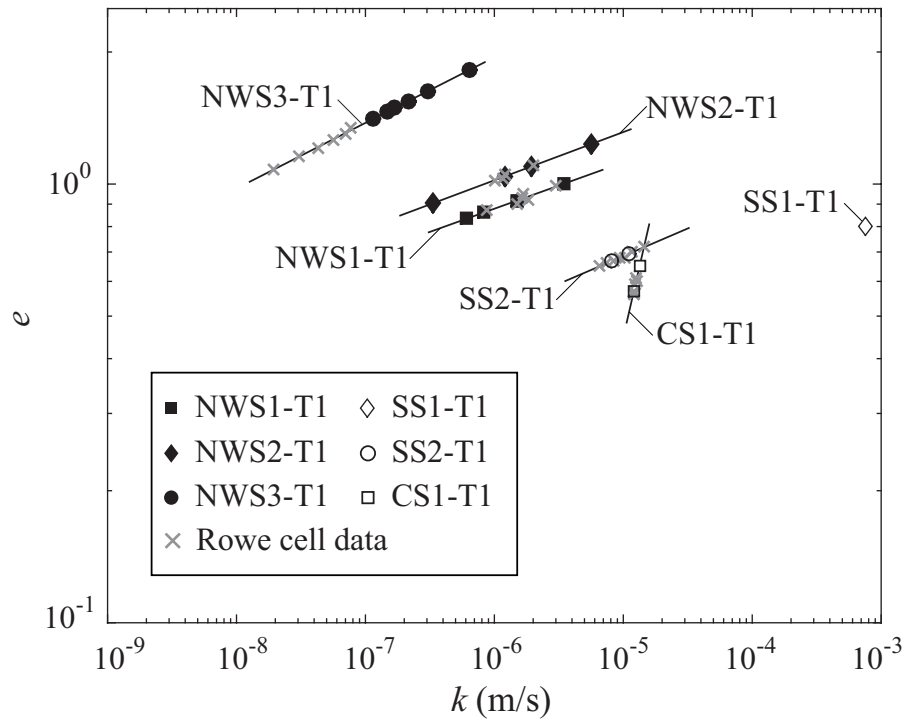

FIG. 7: Permeability against voids ratio with data from Rowe Cell test and least squares fits to this data according to Eq. (8). Using the least squares fits for each sediment, individual permeabilities for each erosion test are deduced using density measurements to determine voids ratio (see Table 2).

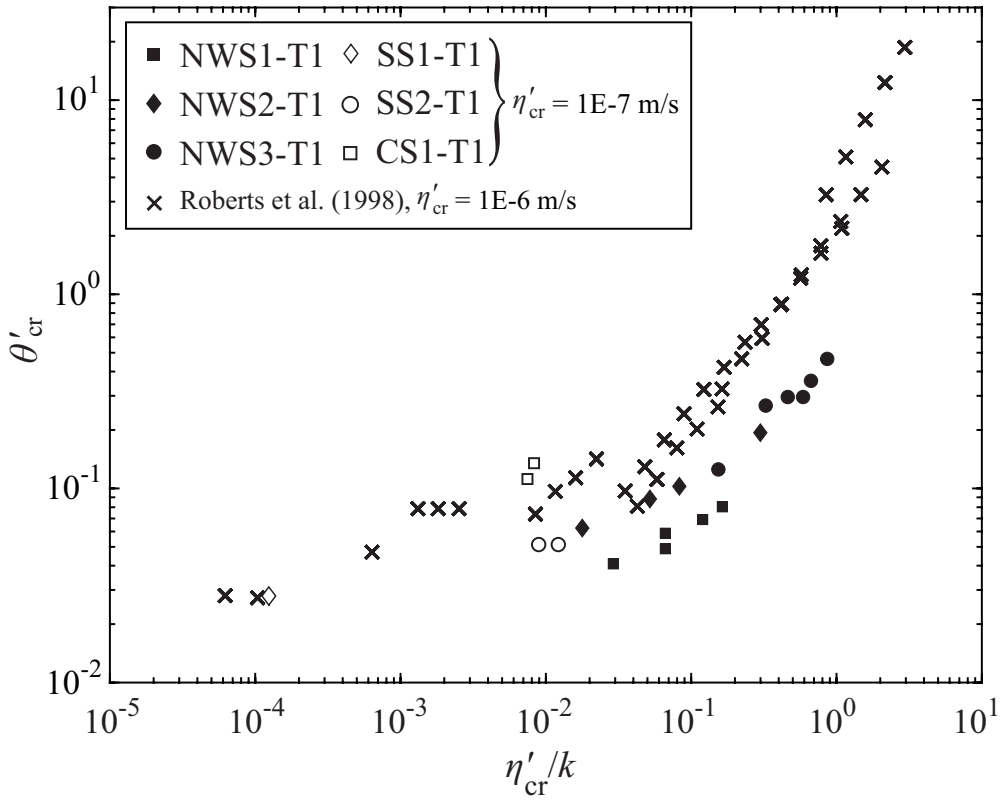

FIG. 8: Permeability against dimensionless threshold shear stress from Table 2 and interpreted data from Roberts et al. (1998).

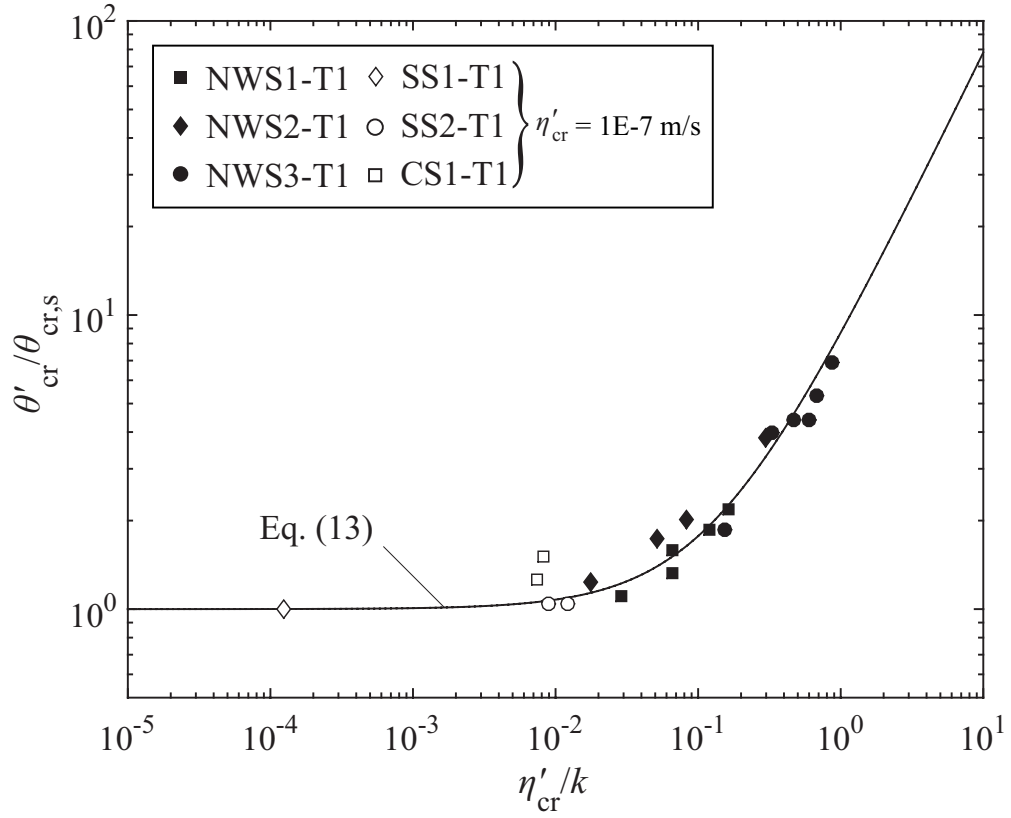

FIG. 9: Calibration of model given in Eq. (13) using erosion data from Table 2 using a reference erosion rate at threshold of 10^{-7} m/s.

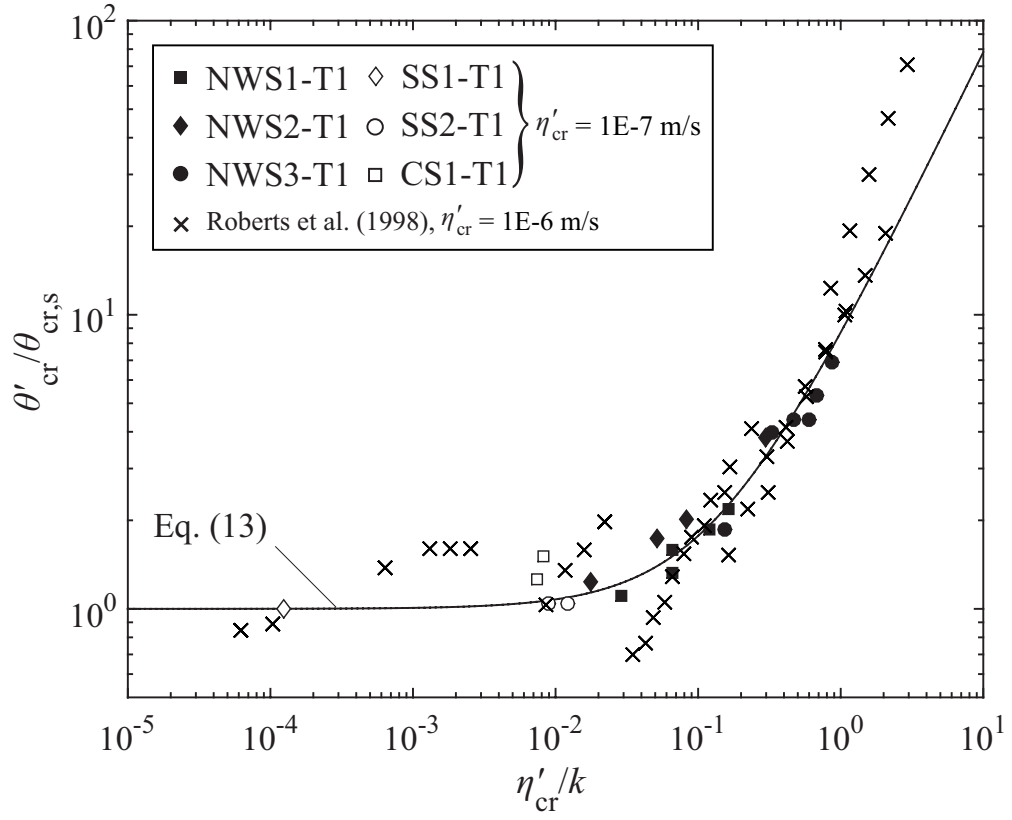

FIG. 10: Comparison of threshold measurements from Roberts et al. (1998) with predictive model given in Eq. (13). The reference erosion rate at threshold is 10^{-6} m/s and 10^{-7} m/s for the measurements from Roberts et al. (1998) and the present study, respectively.

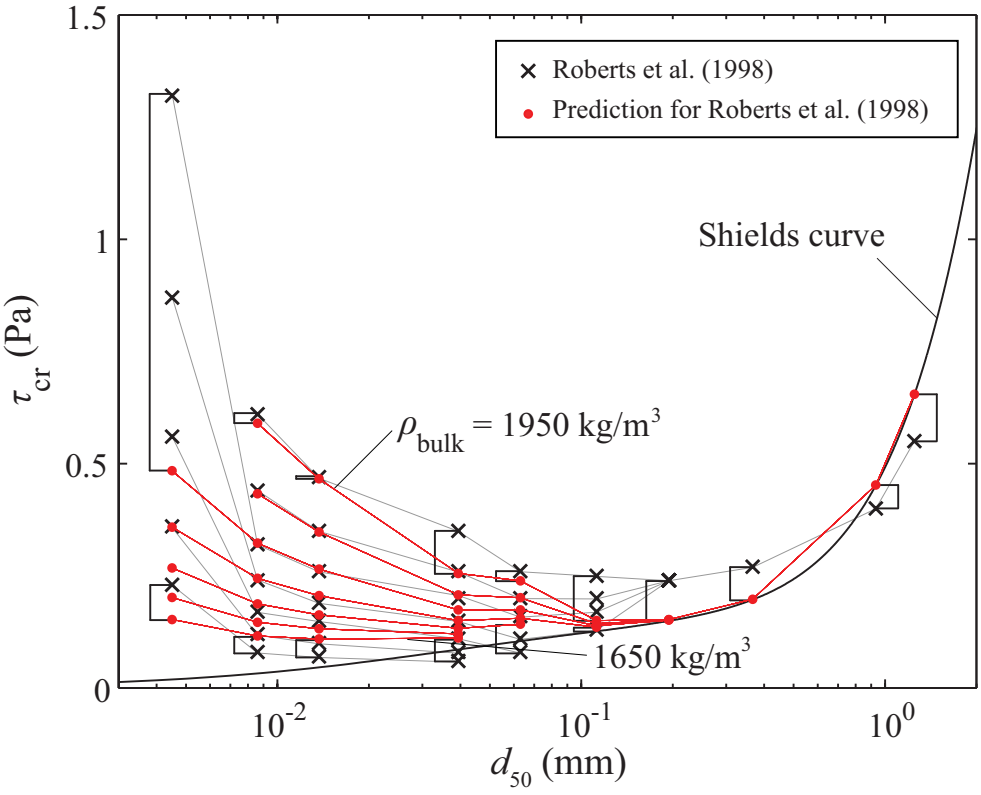

FIG. 11: Comparison of data from Roberts et al. (1998, based on Fig. 6) with predictions using Eq. (13). The diameters used in this figure vary slightly from the original ones as they were taken from digitised PSD curves given in Roberts et al. (1998). These PSD curves were needed to estimate permeability and hence predict the threshold shear stress.

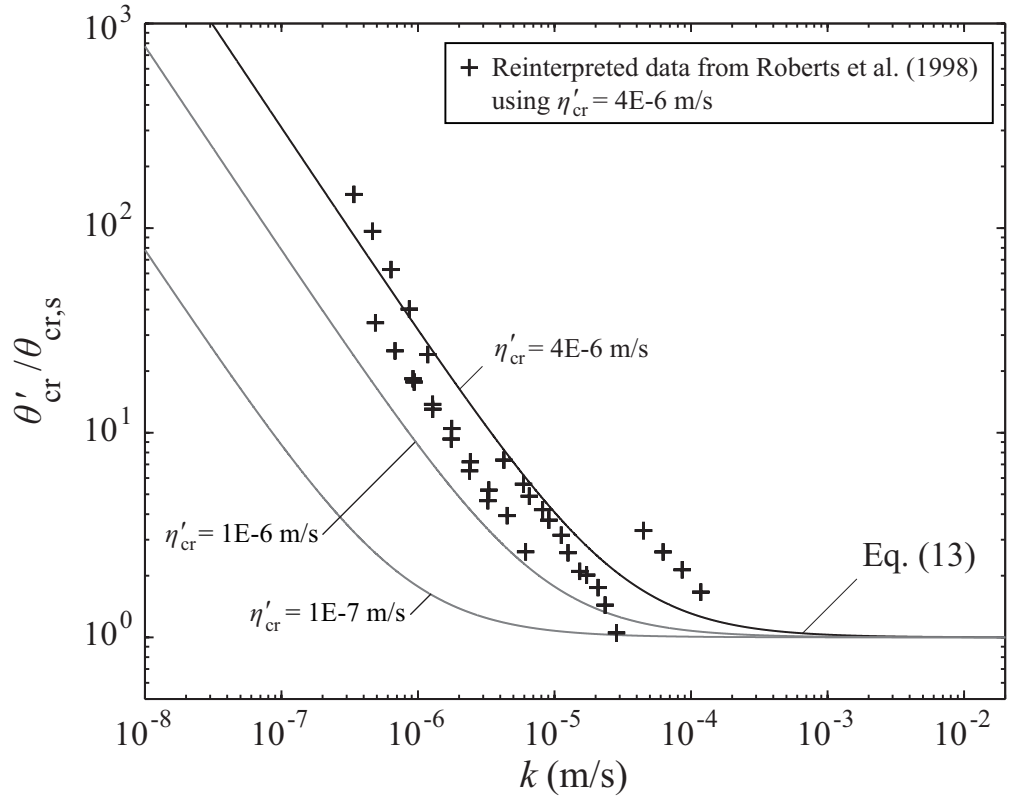

FIG. 12: Assessing the capability of the model by changing the erosion rate defining threshold for data from Roberts et al. (1998) to $\eta'_{cr} = 4 \times 10^{-6}$ m/s. For comparison erosion rates defining threshold are also shown from this study with 10^{-7} m/s and Roberts et al. (1998) with 10^{-6} m/s using Eq. (13). Data for sediments $\geq$ 222 µm are not shown as no accurate approximation of the erosion rate is given in Roberts et al. (1998) making a reinterpretation of the data unattainable.